Available online at www.sciencedirect.com

ScienceDirect

Mendeleev Commun., 2019, **29**, 690–692

Mendeleev Communications

Combustion of ethyl acetate: the experimental study of flame structure and validation of chemical kinetic mechanisms

Ksenia N. Osipova,[a,b] Artem M. Dmitriev,[a,b] Andrey G. Shmakov,[a,b] Oleg P. Korobeinichev,[a] Sergey S. Minaev[c] and Denis A. Knyazkov*[a,b,d]

[a] *V. V. Voevodsky Institute of Chemical Kinetics and Combustion, Siberian Branch of the Russian Academy of Sciences, 630090 Novosibirsk, Russian Federation. E-mail: knyazkov@kinetics.nsc.ru*

[b] *Novosibirsk State University, 630090 Novosibirsk, Russian Federation*

[c] *Institute of Applied Mathematics, Far Eastern Branch of the Russian Academy of Sciences, 690041 Vladivostok, Russian Federation*

[d] *Tomsk State University, 634050 Tomsk, Russian Federation*

DOI: 10.1016/j.mencom.2019.11.030

Mole fraction profiles for reactants, major products, and main combustion intermediates were measured in near-stoichiometric and fuel-rich premixed burner-stabilized flames of ethyl acetate (AcOEt) under atmospheric pressure. Three recent chemical kinetic mechanisms for the AcOEt combustion were validated against the data reported. Their different predictive capabilities were explained using the results of kinetic analysis.

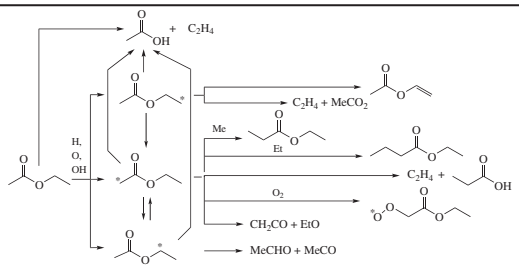

A depletion of natural underground resources (*e.g.*, oil and gas), a permanently increasing demand of the energy, and a negative environmental impact of burning fossil fuels motivate the mankind to shift towards biodiesel fuels since they are renewable, cost-effective and producing low emissions during their combustion. Bioethanol used instead of methanol in the transesterification producing fatty acid ethyl esters can enhance the extent of renewability and, therefore, make ethyl esters more preferable in the biodiesel than methyl esters. The combustion chemistry of ethyl esters bearing alkyl chains of different lengths has been explored quite extensively to clarify how the presence of ester functional group can influence the composition of combustion products and the combustion kinetics as compared to conventional hydrocarbon fuels. At this end, ethyl acetate (AcOEt) has received a great attention, *e.g.*, detailed chemical kinetic mechanisms for its combustion were proposed by different research groups.[1–9] Although the proposed reaction models have been already validated against the series of experimental data for the AcOEt combustion, including those on ignition delays in shock tubes, laminar burning velocity, and speciation measurements during its oxidation in a jet-stirred reactor and low-pressure laminar flames; there is still no established models that can adequately predict the concentrations of intermediates under flame conditions at pressures close to atmospheric or higher, which are the most relevant for practical purposes.

Therefore, this work was aimed at two aspects: (1) to extend the available experimental database for the AcOEt combustion with novel data on the spatial distribution of various intermediates in atmospheric-pressure AcOEt flames and (2) to validate the known chemical kinetic models for the AcOEt combustion against the acquired data in order to elucidate performances and deficiencies of the models. Two premixed burner-stabilized flames diluted with Ar, the near-stoichiometric and fuel-rich ones, were investigated for ascertaining how the available models reproduce the tendencies observed upon changes in the unburnt composition.

Flame sampling molecular beam mass spectrometric setup with soft electron impact ionization[10,11] was used for the examination of laminar premixed flames of two AcOEt/O_2/Ar mixtures stabilized on a Botha–Spalding burner at equivalence ratios $\varphi = 1.13$ (AcOEt/O_2/Ar = 0.037/0.163/0.8, near-stoichiometric) and $\varphi = 1.73$ (AcOEt/O_2/Ar = 0.077/0.223/0.7, fuel-rich).[†] The measured temperature profiles were processed with PREMIX software,[12,13] which was used for the chemical kinetic simulation of distribution of the flame species above the burner. The experimental profiles of mole fractions of the species were compared with those calculated using three detailed reaction mechanisms for the AcOEt combustion proposed by Dayma,[14] Sun,[8] and Ahmed.[9]

Both the measured and calculated temperature and mole fraction profiles of reactants and major flame products in the both near-stoichiometric and fuel-rich flames (Figure S2, Online Supplementary Materials) are in a good agreement with each other. All the mechanisms provided very close predictions for these species.

The primary reaction pathways of AcOEt decomposition in the flames (Figures 1 and S1 for the near-stoichiometric and fuel-rich conditions, respectively) were analyzed according to the approach similar to the reported one.[15,16] Each branch in the diagrams is shown with the numerical values representing the contributions (in different mechanisms) of integrated rate of the each pathway to the total integrated rate of consumption of a particular species in the entire flame.

According to Figure 1, there are two major options for the AcOEt decomposition: (1) H-abstraction reactions with major flame radicals ($H^{\cdot}$, $O^{\cdot}$, $^{\cdot}OH$, *etc.*) to form so-called fuel radicals with unpaired electron located at different positions and (2) unimolecular decomposition *via* a formation of six-membered transition state (not shown in the diagrams) and its further breaking into acetic acid

[†] See Online Supplementary Materials for the experimental procedure and acquired experimental data (mole fraction profiles for the species and temperature profiles).

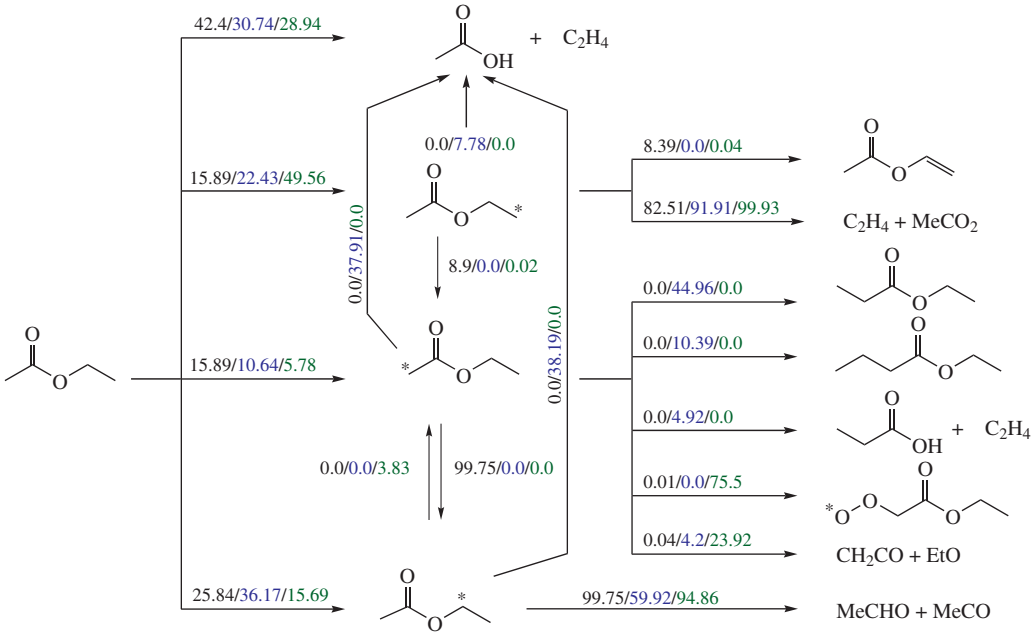

Figure 1 Primary reaction pathways of AcOEt decomposition in the near-stoichiometric flame. Numbers are derived from the analysis of the Dayma, Sun and Ahmed mechanisms (first/second/third, respectively).

and ethylene. The ratio between the rate constants of these primary stages (so-called 'branching ratio') significantly determines the pool of intermediate species formed in the consequent reactions. Note that for the both near-stoichiometric and fuel-rich conditions, the products of decomposition of the fuel radicals were the same.

The contribution of unimolecular AcOEt decomposition to its consumption in the stoichiometric flame is fairly high (30–40%). However, in the case of fuel-rich conditions (see Figure S1), AcOEt decomposes preferably *via* this pathway (its contribution is nearly 90%.) The measurements have qualitatively confirmed this tendency. Figure 2 shows measured and predicted mole fraction profiles of ethylene and acetic acid in both the flames. Thus, the peak mole fraction of AcOH increases along with the equivalence ratio. Under the fuel-rich conditions, all the models have significantly overpredicted the AcOH production, and moreover, the C_2H_4 peak mole fraction was also slightly overpredicted. Since the agreement between modeling and experiment under the near-stoichiometric conditions was satisfactory for AcOH and C_2H_4, the reason for the observed discrepancy in fuel-rich flame might be due to an inaccuracy in the rates of H-abstraction from the fuel.

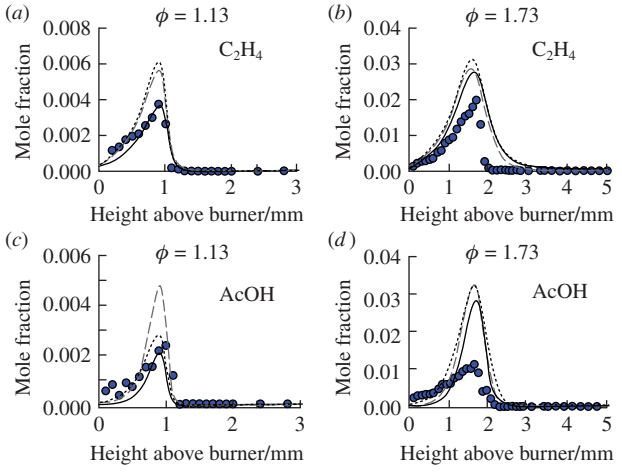

Figure 2 Mole fraction profiles of C_2H_4 and AcOH in the (*a*),(*c*) near-stoichiometric and (*b*),(*d*) fuel-rich flames of AcOEt. Symbols correspond to the experiment, and lines represent the modeling (solid, dashed and dotted lines for the Dayma, Sun and Ahmed mechanisms, respectively).

Indeed, the different mechanisms exhibit significantly different contributions of H-abstraction reactions to the formation of specific fuel radicals. This indicates the remaining lack of understanding of these elementary processes. Moreover, possible reactions of isomerization between the fuel radicals are differently represented by the mentioned mechanisms. In particular, $^{\cdot}CH_2C(O)OEt$ radical almost completely isomerizes into $^{\cdot}CH(Me)OAc$ according to the Dayma mechanism, while the two other models do not contain such a pathway. The latter radical (see Figure 1) undergoes mostly a β-scission reaction to give acetaldehyde and $^{\cdot}C(O)Me$ according to all the mechanisms. The analysis has also revealed that this reaction represents a major pathway of the acetaldehyde formation. Our experimental data on acetaldehyde were best described by the Dayma mechanism, while the two other mechanisms underpredicted its peak mole fraction, indicating indirectly that the mentioned isomerization plays an important role in the AcOEt combustion (Figure 3). Unfortunately, we were unable to detect any major species in the flames, which are supposed to be primary decomposition products of $^{\cdot}CH_2C(O)OEt$ radical. In particular, these products are propyl acetate, butyl acetate, and propionic acid according to Sun mechanism, while according to the Ahmed mechanism, $^{\cdot}CH_2C(O)OEt$ radical is mostly consumed in the reaction with molecular O_2 to give $^{\cdot}OOCH_2C(O)OEt$.

However, the mass peak of 42 corresponding to propene and ketene was successfully detected (see Figure S3). All the models provide close predictions for propene in the flames, but differently predict ketene. According to Sun and Ahmed mechanisms, ketene is mostly formed *via* the reaction $^{\cdot}CH_2C(O)OH \rightarrow CH_2CO + {}^{\cdot}OH$.

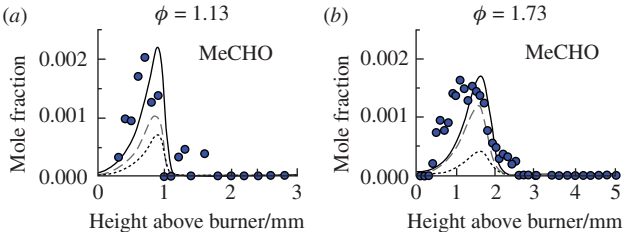

Figure 3 Mole fraction profiles of acetaldehyde in the (*a*) near-stoichiometric and (*b*) fuel-rich flames of AcOEt. Symbols correspond to the experiment, and lines represent the modeling (solid, dashed and dotted lines for the Dayma, Sun and Ahmed mechanisms, respectively).

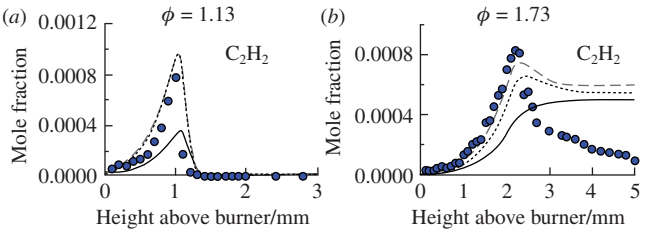

Figure 4 Mole fraction profiles of acetylene in the (*a*) near-stoichiometric and (*b*) fuel-rich flames of AcOEt. Symbols correspond to the experiment, and lines represent the modeling (solid, dashed and dotted lines for the Dayma, Sun and Ahmed mechanisms, respectively).

The radical, ketene precursor, is formed mainly due to the reaction of H-abstraction from AcOH by flame radicals ($H^{\cdot}$, $O^{\cdot}$, $^{\cdot}OH$). Therefore, in the two mentioned mechanisms, production of ketene is closely related to the AcOH formation, and they overpredict the ketene peak mole fraction (as well as AcOH), especially in the fuel-rich flame. Figure 3 shows that the Dayma mechanism predicts acetaldehyde peak mole fraction better than the other mechanisms. According to this mechanism, ketene is mostly formed *via* the reaction $^{\cdot}CH_2CHO \rightarrow CH_2CO + H^{\cdot}$. The $^{\cdot}CH_2CHO$ radical is a primary product of H-abstraction from acetaldehyde, which is consequently a primary precursor of ketene. Therefore, the ketene formation pathways (and corresponding reaction rate constants) suggested by Dayma seem more adequate than those according to the Sun and Ahmed mechanisms.

The Dayma mechanism was developed using the previous mechanisms elaborated for oxygenated fuels, in particular, on the well validated mechanism for *n*-butanol combustion. *Per contra*, the Sun and Ahmed mechanisms are based on the kinetic mechanisms for the combustion of alkanes. Thus, the kinetics of short oxygenated compounds such as aldehydes and ketones in the flames of AcOEt is better described by Dayma mechanism.

In the near-stoichiometric flame, $H^{\cdot}$ and $^{\cdot}OH$ radicals were also detected, and their mole fraction profiles were predicted well according to all the three mechanisms (Figure S4). The content of $Me^{\cdot}$ radical was measured in both flames, and its mole fraction profiles were also reproduced by all the mechanisms, although the Sun model was slightly better in predicting $Me^{\cdot}$, especially under the fuel-rich conditions. The analysis of rates of $Me^{\cdot}$ production and consumption has revealed that the rate constant for the reaction $Me^{\cdot} + O^{\cdot\cdot} \rightarrow CH_2O + H^{\cdot}$ (the major path of methyl consumption) at ~1400 K (where the maximum of $Me^{\cdot}$ mole fraction is attained) in the case of Sun mechanism is 5 times higher than in two others. This may explain the fact that the Sun mechanism is the best one for the reproduction of C_2H_6 mole fraction (Figure S5), because it is formed essentially *via* the recombination of methyl radicals.

Formaldehyde peak mole fraction remained almost unchanged upon increasing the equivalence ratio (Figure S6). The reaction between methyl radical and oxygen atom ($Me^{\cdot} + O^{\cdot\cdot} \rightarrow CH_2O + H^{\cdot}$) is the main pathway of formaldehyde formation, whereas the reaction of H-abstraction from formaldehyde ($CH_2O + O^{\cdot\cdot} \rightarrow HC^{\cdot}O + {}^{\cdot}OH$) is its major consumption pathway. All the mechanisms provide very similar prediction of CH_2O profiles in both the flames. Methane mole fraction profiles (Figure S7) were predicted quite well according to all the mechanisms, however in the case of fuel-rich flame, the Ahmed mechanism overpredicted its mole fraction in the post-flame zone.

The Dayma mechanism underpredicted the peak mole fraction of acetylene in the near-stoichiometric flame (Figure 4), whereas the two other models predicted the C_2H_2 profile very accurately. The comparison of major reaction pathways of C_2H_2 production and consumption according to the different mechanisms revealed that the rate constant for the major reaction of C_2H_2 formation ($^{\cdot}C_2H_3 + H^{\cdot} \rightarrow C_2H_2 + H_2$) according to the Dayma mechanism is ~3 times lower than that in other mechanisms, while the rate parameter of other reactions involving C_2H_2 was very similar in all the three mechanisms. This may explain the observed underprediction of C_2H_2 mole fraction according to the Dayma mechanism. However, under the fuel-rich conditions, all the mechanisms did not reproduce the C_2H_2 profile even qualitatively: the models did not predict a drop in its mole fraction in the post-flame zone. Nevertheless, the Ahmed and Sun models accurately predicted its peak mole fraction in the fuel-rich flame. The disagreement between the modeling and experiment for C_2H_2 in the post-flame zone is a well-known difficulty for the fuel rich flames, which was also encountered in our previous works,[10,11] thus indicating that acetylene oxidation chemistry deserves a more detailed analysis.

In summary, the obtained experimental data on the structure of near-stoichiometric and fuel rich flames of AcOEt revealed the performances and deficiencies of available chemical kinetic mechanisms for AcOEt combustion. The Dayma mechanism demonstrated better predictive capabilities for short oxygenated compounds, while the Sun and Ahmed mechanisms better reproduced the mole fraction profiles for light hydrocarbons. The observed discrepancies arise from different origins of the mechanisms, and they indicate once again that there is no common agreement on the formation kinetics for short oxygenated and C_1–C_4 hydrocarbons. The reported data can be used for further improvement of detailed chemical kinetic models for high-temperature AcOEt oxidation.

Online Supplementary Materials

Supplementary data associated with this article can be found in the online version at doi: 10.1016/j.mencom.2019.11.030.

References

1 L. Gasnot, V. Decottignies and J. F. Pauwels, *Fuel*, 2004, **83**, 463.
2 L. Gasnot, V. Decottignies and J. F. Pauwels, *Fuel*, 2005, **84**, 505.
3 B. Akih-Kumgeh and J. M. Bergthorson, *Energy Fuels*, 2011, **25**, 4345.
4 W. Ren, R. M. Spearrin, D. F. Davidson and R. K. Hanson, *J. Phys. Chem. A*, 2014, **118**, 1785.
5 C. K. Westbrook, W. J. Pitz, P. R. Westmoreland, F. L. Dryer, M. Chaos, P. Osswald, K. Kohse-Höinghaus, T. A. Cool, J. Wang, B. Yang, N. Hansen and T. Kasper, *Proc. Combust. Inst.*, 2009, **32**, 221.
6 Y. L. Wang, D. J. Lee, C. K. Westbrook, F. N. Egolfopoulos and T. T. Tsotsis, *Combust. Flame*, 2014, **161**, 810.
7 T. Badawy, J. Williamson and H. Xu, *Fuel*, 2016, **183**, 627.
8 W. Sun, T. Tao, R. Zhang, H. Liao, C. Huang, F. Zhang, X. Zhang, Y. Zhang and B. Yang, *Combust. Flame*, 2017, **185**, 173.
9 A. Ahmed, W. J. Pitz, C. Cavallotti, M. Mehl, N. Lokachari, E. J. K. Nilsson, W. J. Yang, A. A. Konnov, S. W. Wagnon, B. Chen, Z. Wang, S. Kim, H. J. Curran, S. J. Klippenstein, W. L. Roberts and S. M. Sarathy, *Proc. Combust. Inst.*, 2019, **37**, 419.
10 I. E. Gerasimov, D. A. Knyazkov, S. A. Yakimov, T. A. Bolshova, A. G. Shmakov and O. P. Korobeinichev, *Combust. Flame*, 2012, **159**, 1840.
11 A. M. Dmitriev, D. A. Knyazkov, T. A. Bolshova, A. G. Shmakov and O. P. Korobeinichev, *Combust. Flame*, 2015, **162**, 1964.
12 R. J. Kee, J. F. Grcar, M. D. Smooke, J. A. Miller and E. Meeks, *PREMIX: a Fortran Program for Modeling Steady Laminar One-Dimensional Premixed Flames*, Livermore, CA, 1985.
13 R. J. Kee, F. M. Rupley and J. A. Miller, *Chemkin-II: A Fortran Chemical Kinetics Package for the Analysis of Gas-Phase Chemical Kinetics*, Livermore, CA, 1989.
14 G. Dayma, F. Halter, F. Foucher, C. Togbé, C. Mounaim-Rousselle and P. Dagaut, *Energy Fuels*, 2012, **26**, 4735.
15 I. E. Gerasimov, D. A. Knyazkov, A. M. Dmitriev, L. V. Kuibida, A. G. Shmakov and O. P. Korobeinichev, *Combust. Explos. Shock Waves*, 2015, **51**, 285.
16 A. M. Dmitriev, K. N. Osipova, D. A. Knyazkov, I. E. Gerasimov, A. G. Shmakov and O. P. Korobeinichev, *Combust. Explos. Shock Waves*, 2018, **54**, 125.

Received: 8th May 2019; Com. 19/5917